

Isotherms, kinetics, and thermodynamics of methionine adsorption onto poorly crystalline hydroxyapatite with different Ca/P ratios

Abdelhadi El Rhilassi^{a,b*}, Oumaima Oukkass^b and Mounia Bennani-Ziatni^b

^aTraining Center of Education Inspectors (CFIE) of Rabat, Morocco

^bLaboratory of Organic Chemistry, Catalysis and Environment, Department of Chemistry, Faculty of Sciences, Ibn Tofail University, BP 242, 14000, Kenitra, Morocco

CHRONICLE

Article history:

Received December 25, 2022

Received in revised form

January 28, 2023

Accepted April 26, 2023

Available online

April 26, 2023

Keywords:

Hydroxyapatite

Methionine

Kinetic

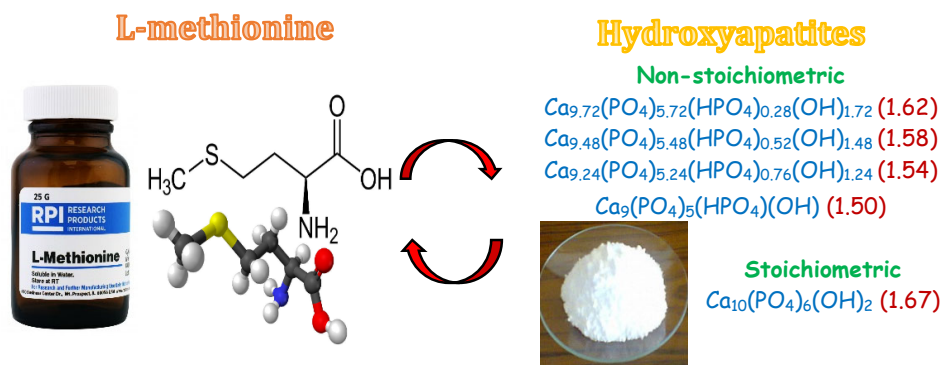
Isotherm

Thermodynamic

ABSTRACT

The adsorption properties of hydroxyapatite of low crystallinity towards methionine have been examined. The chemical composition of hydroxyapatite was taken as an experimental variable in order to have a point of view on the parameters of the adsorption process and the mechanisms established between adsorbent-adsorbate. The adsorption kinetics are relatively fast, and the high amounts adsorbed at saturation are obtained for non-stoichiometric hydroxyapatite, containing more HPO_4^{2-} ions and having a high specific surface area. The good agreement of the experimental data with kinetic models confirms that the mechanism can be perfectly described by pseudo-second-order kinetics. Adsorption isotherm models show that Langmuir's model gives a better fit of experimental data compared to that of Freundlich, Temkin and Dubinin-Kaganer-Radushkevich. Fourier transform infrared spectroscopy confirmed the interaction between the $-\text{COO}^-$ ions of methionine and the Ca^{2+} ions of hydroxyapatite. The thermodynamic parameters, the isoelectric point of methionine and the point of zero charge of hydroxyapatite with different Ca/P ratios show that the adsorption process is considered spontaneous, exothermic and often controlled by physisorption with interactions electrostatic.

© 2023 by the authors; licensee Growing Science, Canada.



Graphical abstract

1. Introduction

The phenomena that occur at the interface between apatitic calcium phosphates and the surrounding environment have been the subject of many studies in reason of the biological properties of these biomaterials, and also their involvement in diverse fields (medicine, biotechnology, biology, environment, etc.).¹⁻³ These compounds, especially hydroxyapatite which

* Corresponding author. Tel : +212 6 62 13 13 72

E-mail address aelrhilassi@gmail.com (A. El Rhilassi)

has been widely studied and used clinically, can bind biological molecules and macromolecules such as amino acids,⁴ proteins,⁵ etc. This is due to its excellent biocompatibility, bioactivity and osteoconductivity and its chemical and structural similarity with natural bone minerals. Nowadays, these phosphates are also used for drug delivery applications and controlled antibiotic release for treating, for example, fracture-related infections in osteoporotic bone, and bone defects.^{6,7}

One of the most interesting properties of apatites is their ability of the lattice to accept ionic substituents and vacancies. Due to this property, non-stoichiometric apatites are quite easy to synthesize.⁸ Most exchange reactions between adsorbate and adsorbent are related to the exchange of surface ions. These exchanges are made possible because of the high specific surface area of the apatites used but also, essentially, because of the existence of a hydrated layer on the apatite surface containing loosely bound ions.⁹

Because of a lower Ca/P ratio than stoichiometric hydroxyapatite, calcium-deficient hydroxyapatite benefits from a higher solubility and consequently, it biologically appears more bioactive than stoichiometric hydroxyapatite.^{10,11} Therefore calcium-deficient hydroxyapatite, whose composition and structure are very close to the natural bone mineral,¹² is of greater biological interest than stoichiometric hydroxyapatite and is a suitable candidate for bone regeneration.¹³

Despite research on the surface properties of apatites, their mode of interaction with the surrounding environment remains poorly understood (adsorption, desorption, etc.), due to the complexity of the adsorbate-adsorbent system, on the one hand, and poorly controlled conditions, on the other hand.

This work contributes to investigating the parameters involved in the adsorption of the amino acid L-methionine on synthetic hydroxyapatites, which are well characterized. These parameters which are related to isotherm models, kinetic models and thermodynamic properties can help to understand the mechanisms which govern the phenomena at the interface between hydroxyapatite of various compositions and L-methionine of character hydrophobic, and also to determine the nature of the adsorption process. For this reason, the chemical composition of the adsorbents was taken as an experimental variable.

In this work, we are interested in testing two types of poorly crystalline hydroxyapatites of different compositions, which are prepared by chemical precipitation technique at pH~7.4 and at 298 K. They are (1) stoichiometric hydroxyapatite with Ca/P = 1.67 of formula $\text{Ca}_{10}(\text{PO}_4)_6(\text{OH})_2$ and (2) non-stoichiometric calcium-deficient hydroxyapatites of $1.5 \leq \text{Ca/P} < 1.67$ can be described by the following formula $\text{Ca}_{10-x}(\text{PO}_4)_{6-x}(\text{HPO}_4)_x(\text{OH})_{2-x}$ with $0 < x \leq 1$.¹⁴ The amount of HPO_4^{2-} ions in these compounds will be considered as variable experimental towards the methionine reactivity and for the adsorption process under physiological conditions of pH~7 and T= 310K.

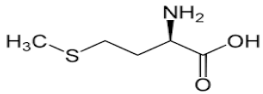
In this paper, hydroxyapatite samples were prepared by varying the Ca/P ratio. As a consequence, samples with different stoichiometries were obtained and characterized.

2. Material and methods

2.1 Adsorbate

L-Methionine is one of nine essential amino acids that cannot be made by the human body, it must be obtained from dietary sources. It contains sulfur and is found in many proteins, including dietary proteins. The properties of L-Methionine are illustrated in **Table 1**,^{15,16} its infrared spectrum is shown in **Fig 1**.

Table 1. Properties of L-Methionine.^{15,16}

Amino acid	L-Methionine
Chemical structure	
Chemical formula	$\text{C}_5\text{H}_{11}\text{NO}_2\text{S}$
IUPAC Name	2-Amino-4-(methylthio)butanoic acid
Hydrophobicity	hydrophobic (non-polar)
Acidity (pKa) at 298 K	2.28 (carboxyl), 9.21 (amino)
Isoelectric point (pI) at 298 K	5.74
Molecular weight (g/mol)	149.21
Density at 293 K (g/cm^3)	1.34
Appearance	White crystalline powder
Solubility in water at 298 K (g/L)	56.6

The infrared spectrum of methionine shows strong bands located between 1000 and 1350 cm^{-1} attributed to the C-N bond of the primary amine.¹⁷ The shoulder between 2500 and 3000 cm^{-1} corresponds to the O-H bond.¹⁷ There are also bands observed at 1580 and 1607 cm^{-1} characteristic of the C=O bond as well as at 3300 cm^{-1} a band corresponding to the N-H bond.¹⁷ Other bands observed between 2500 and 2600 cm^{-1} and between 650 and 750 cm^{-1} are successively attributed to the S...H and C-S bonds existing in the methionine molecule.¹⁸

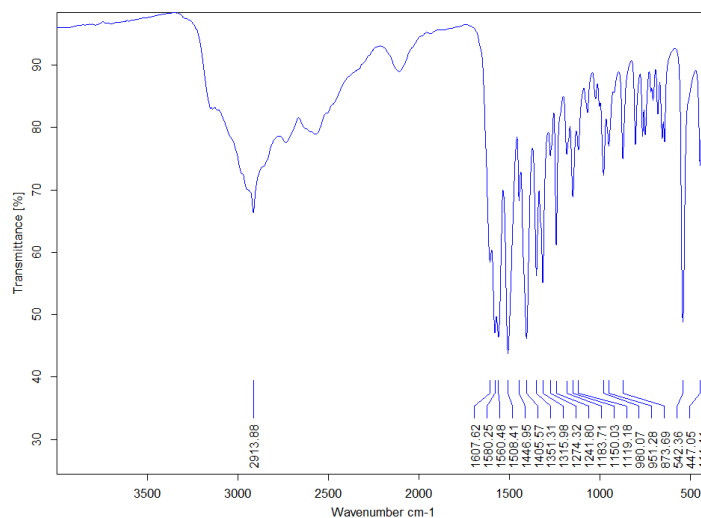


Fig. 1. Infrared spectra of L-Methionine

2.2 Adsorbents

2.2.1 Preparation

The adsorbents are prepared by co-precipitation method between two solution A [calcium nitrate $\text{Ca}(\text{NO}_3)_2 \cdot 4\text{H}_2\text{O}$ (Riedel- de Haën -Germany)] and B [di-ammonium hydrogenphosphate $(\text{NH}_4)_2\text{HPO}_4$ (Riedel-de Haën, Germany)]. In this preparation, the Ca/P ratio is varied between 1.50 and 1.67 by varying the amount of phosphorus between 45 and 50 mmoles, while maintaining the amount of calcium constant and equal to 75 mmoles. The co-precipitation is carried out at $T \sim 310$ K by rapidly pouring, with stirring, solution (A) into solution (B). The pH value was adjusted to ~ 7.4 by adding a few drops of concentrated ammonia NH_4OH . After stirring (500 rpm) for 2 hours, the co-precipitates formed are filtered through Büchner, then washed with distilled water, dried in an oven at 70°C for 48 hours, ground and sieved ($<210 \mu\text{m}$).

2.2.2 Characterization of synthesized apatites

The powders obtained are characterized by physicochemical analysis. The calcium content was determined by complexometry with Ethylene Diamine Tetra Acetic Acid (EDTA) and the phosphate ion content by spectrophotometry of phospho-vanado-molybdic acid. The values obtained of Ca/P molar ratio of synthetic apatites are between 1.50 and 1.67 (**Table 2**).

The specific surface area was determined through to the Saers method.¹⁹ 0.5 g of adsorbent sample was acidified with 0.1 M HCl at pH between 3 and 3.5, the volume was made up to 50 mL with deionized water after addition of 10.0 g of NaCl. The solution obtained was titrated with 0.1 M NaOH in a thermostatic bath at 298 ± 0.5 K. The specific surface area is calculated from the following equation:

$$S (\text{m}^2/\text{g}) = 32V_{(\text{NaOH})} - 25 \quad (1)$$

Where, $V_{(\text{NaOH})}$ is the volume of NaOH required to rise the pH from 4.0 to 9.0 (mL). The specific surface found is between 75 and 157 m^2/g (**Table 2**), it increases when the Ca/P ratio decreases, and it is important for the compound of Ca/P=1.50 which contains more HPO_4^{2-} ions.

The zero-point charge (pH_{PCZ}) of the apatites was determined by a simple technique,²⁰ 0.2 g powder placed in beakers containing 20 mL of 0.01 M NaCl solution. The initial pH of these solutions is adjusted from 4 to 10 by adding sodium hydroxide solution (0.1 M) or hydrochloric acid solution (0.1 M). After 48 hours of stirring speed (250 rpm) at ambient temperature, the final pH is measured. The pH_{PCZ} was determined by plotting $\text{pH}_{(\text{final})} - \text{pH}_{(\text{initial})}$ against the $\text{pH}_{(\text{initial})}$ (**Fig. 2**). In the present study, the pH_{pzc} of the synthetic apatites is between 6.55 and 6.9 (**Table 2**). The reports atomics Ca/P obtained allows us to calculate the x values by the following relationship:

$$x = 10 - 6 (\text{Ca/P}) \text{ with } 0 \leq x \leq 1 \quad (2)$$

The chemical formulas of synthesized apatites are illustrated in **Table 2**.

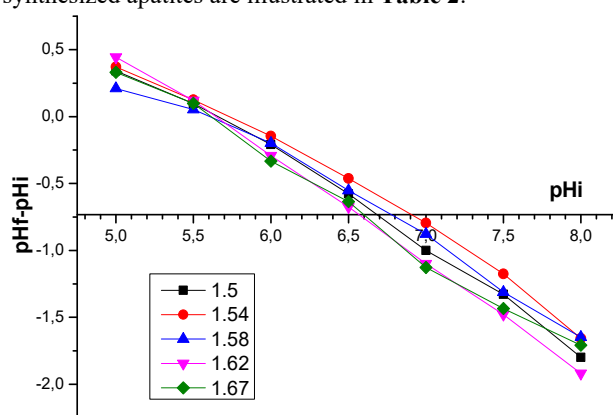


Fig. 2. pH_{ZPC} of synthesized hydroxyapatites of Ca/P 1.50, 1.54, 1.58, 1.62 and 1.67

Table 2. Chemical compositions, specific surface areas, pH_{ZPC} and chemical formulas of synthetic hydroxyapatites in $0 \leq x \leq 1$.

Ca (mmol)	P (mmol)	Ca/P ± 0.01	x	Chemical formula	pH_{ZPC}	specific surface area (m^2/g) ± 0.05
10.5	6.30	1.67	0.00	$\text{Ca}_{10}(\text{PO}_4)_6(\text{OH})_2$	6.60	75
10.6	6.55	1.62	0.28	$\text{Ca}_{9.72}(\text{PO}_4)_{5.72}(\text{HPO}_4)_{0.28}(\text{OH})_{1.72}$	6.55	88
10.7	6.80	1.58	0.52	$\text{Ca}_{9.48}(\text{PO}_4)_{5.48}(\text{HPO}_4)_{0.52}(\text{OH})_{1.48}$	6.80	101
10.8	7.02	1.54	0.76	$\text{Ca}_{9.24}(\text{PO}_4)_{5.24}(\text{HPO}_4)_{0.76}(\text{OH})_{1.24}$	6.90	114
10.9	7.29	1.50	1.00	$\text{Ca}_9(\text{PO}_4)_5(\text{HPO}_4)(\text{OH})$	6.70	157

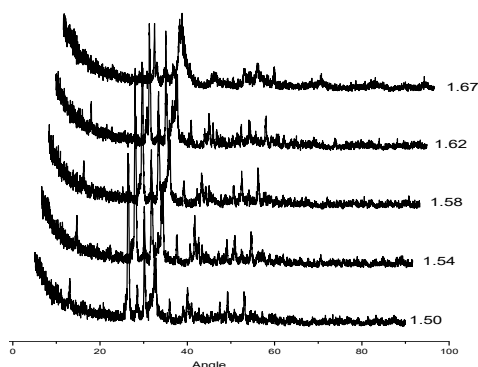


Fig. 3. XRD patterns of synthesized apatites of Ca/P 1.50, 1.54, 1.58, 1.62 and 1.67

X-ray powder diffraction (XRD) pattern was analyzed using X'Pert PRO (Germany) X-ray diffractometer with Cu K α radiation. X-ray diffraction of synthesized adsorbents of Ca/p between 1.50 and 1.67 (**Fig. 3**) shows broad and poorly resolved lines characteristic of poorly crystalline apatites like the mineral phase of calcified tissue.²¹

Infrared spectroscopy (FT-IR) was carried out by using 89 VERTEX 70/70 V FT-IR spectrometers (Bruker Optics). The spectra of synthesized adsorbents of Ca/p between 1.50 and 1.67 (**Fig. 4**) reveal broad and poorly resolved bands confirming the poor crystallinity of these hydroxyapatites. The attributions as well as the relative intensities of the vibration bands observed are grouped together in **Table 3**. We noted that the bands corresponding to the OH^- and PO_4^{3-} groups^{22,23} intensify when the Ca/P ratio increases from 1.50 to 1.67.

The presence of HPO_4^{2-} ions,²⁴ substituted for the PO_4^{3-} groups, attests that the apatite synthesized is non-stoichiometric (deficient in calcium ions). The intensity of this band decreases when the Ca/P ratio increases from 1.50 to 1.67 and disappears for the stoichiometric compound of Ca/P ratio=1.67 (**Fig. 4(d)**).

Table 3. FTIR absorption bands of synthesized hydroxyapatites of Ca/P between 1.50 and 1.67, dried at 80°C.

Absorption bands, (cm^{-1})	Chemical groups
630 ; 1630	OH^-
880	HPO_4^{2-}
560 ; 600 ; 960 ; 1020 ; 1120	PO_4^{3-}
2600 - 3600	H_2O

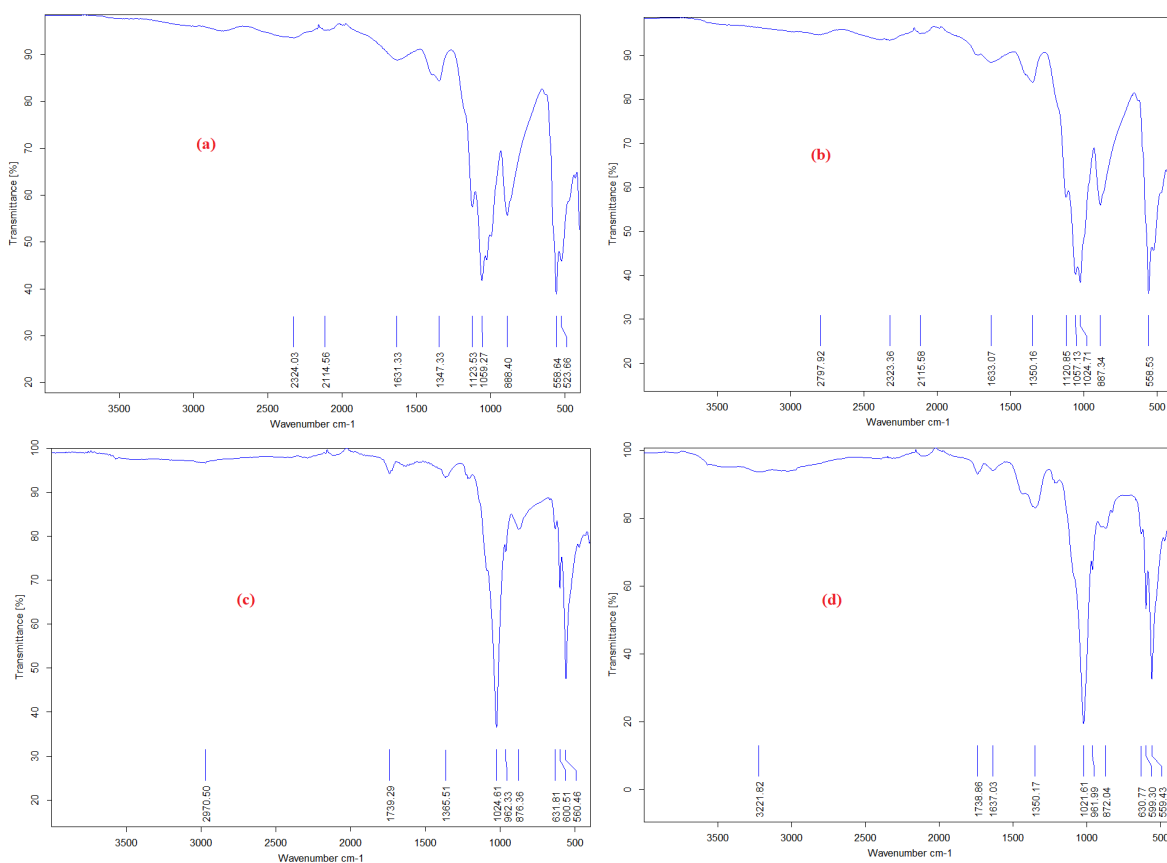


Fig. 4. FTIR spectra of synthesized hydroxyapatites of Ca/P 1.54(a), 1.58(b), 1.62(c) and 1.67(d)

2.3 Adsorption studies

The adsorption of methionine was investigated by batch experiments. For preparing the samples, 200 mg of powder apatite was added to 10 mL of methionine solution. After stirring for 2 min at the speed of 400 rpm, the mixtures of adsorbate and adsorbent are placed in a thermostatic bath at a physiological temperature of 310 K for different contact times. Solutions collected were filtered by the fritted glass (Frit Glass N°4), and the solids obtained were dried in the oven at 343 K for 24 h. All solutions were examined by determining the equilibrium concentration using a UV-vis spectrophotometer (Model 3100, Japan) at 400 nm. The amount of adsorbed methionine per unit of apatite mass was calculated using the expression :

$$q_e (\text{mg/g}) = V \cdot (C_0 - C_e) / m \quad (3)$$

where C_0 , initial concentration of methionine (mg/ml); C_e , concentration of methionine in solution at equilibrium time; V , solution volume (L) and m , mass of adsorbent (g).

The kinetic experiments were carried out for different contact times (0.5, 1, 3, 5, 8, 18 and 24h) with initial methionine concentration ($C_0 = 14.9$ mg/L), at initial solution pH (~ 7) and at 310 K. Adsorption isotherms were studied on methionine solutions with varying concentrations from 14.9 to 745 mg/L at 310 K and at initial solution pH (~ 7). The thermodynamic study was investigated at three different temperatures, 298, 310, and 318 K on methionine solutions with initial concentration $C_0 = 149.2$ mg/L and initial solution pH (~ 7).

3. Results and discussion

3.1 Study of the solutions

3.1.1 Adsorption kinetics

The evolution of the amounts of methionine adsorbed q_{ads} (mg/g) on hydroxyapatites of Ca/P between 1.50 and 1.67 versus time, t (h) are shown in **Fig.5**. The adsorbed amount of methionine increases from the beginning of the adsorbent-adsorbate contact and after five hours of contact, the quantity adsorbed remains constant as a function of time, thus showing that equilibrium is reached and that the adsorption kinetics is fast. The adsorption kinetics is influenced by the composition of the hydroxyapatite. Indeed, the calcium-deficient hydroxyapatites of Ca/P ratio between 1.50 and 1.62 are more

adsorbents than stoichiometric hydroxyapatite of Ca/P=1.67 ; e.g, the maximum amount absorbed at saturation $q_e(m)$ increases from 6.4 mg/g for non-stoichiometric hydroxyapatite of Ca/p= 1.50 containing more HPO_4^{2-} ions to 5.44mg/g for stoichiometric hydroxyapatite of Ca/p= 1.67 exempt of HPO_4^{2-} ions.

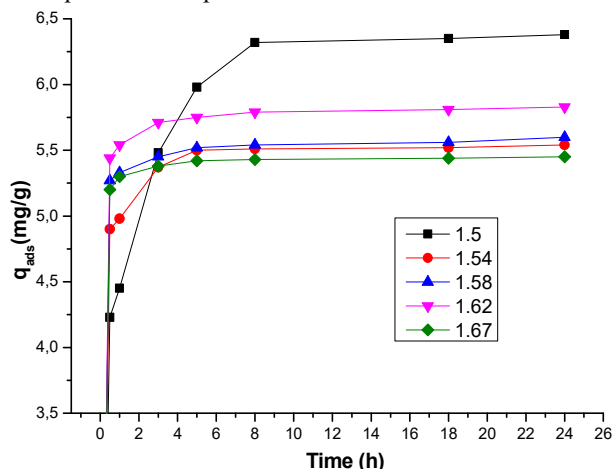


Fig. 5. Adsorption kinetics of methionine on hydroxyapatites of Ca/P between 1.50 and 1.67 (solid quantity : 20 mg, initial methionine concentration : 149.2 mg/L, initial pH~7, at 310 K)

The kinetics of methionine adsorption onto hydroxyapatite with varying Ca/P ratios have been determined by using four kinetic models : the pseudo-first order, pseudo-second order, Elovich kinetic, and the Weber-Morris intraparticle diffusion model.

Pseudo-first order model. This model is given by Lagergren,²⁵ and its equation is expressed as ;

$$dq_t/dt = K_1(q_e - q_t) \quad (4)$$

The integration of this equation for the following boundary conditions ($t = 0, q_t = 0$; $t = t, q_t = q_t$) leads to the following linear form :

$$\ln(q_e - q_t) = \ln q_e - K_1 t \quad (5)$$

where, $q_e(mg/g)$ is the amount of the methionine adsorbed per unit weight of the hydroxyapatite at equilibrium, $q_t(mg/g)$ is the amount adsorbed at time t (h) and $K_1(h^{-1})$ is the rate constant for pseudo-first order rate expression. The plots between $\ln(q_e - q_t)$ versus t at 310 K for hydroxyapatites of Ca/P=1.50, 1.54, 1.58, 1.62 and 1.67 are shown in **Fig. 6**. The values of K_1 and q_e are calculated, respectively, from the slope and intercept derived from these plots $\ln(q_e - q_t) = f(t)$ and are given in **Table 4**. The large difference between experimental $q_e(exp)$ and calculated $q_e(cal)$ values of the maximum amount adsorbed and the low values of correlation coefficient R^2 (**Table 4**) indicates that pseudo-first order model is not suitable to explain the reaction mechanisms for the methionine adsorption by these five hydroxyapatites.

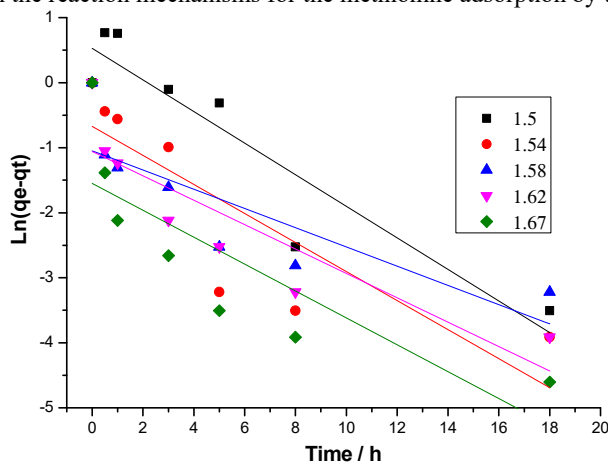


Fig. 6. Pseudo-first-order kinetics for adsorption of methionine on hydroxyapatites of Ca/P between 1.50 and 1.67

Pseudo-second order model. The kinetic expression of this model is proposed by Ho and McKay,²⁶ and its equation is expressed as ;

$$dq_t/dt = K_2(q_e - q_t)^2 \quad (6)$$

After integration and applying boundary conditions, $t = 0$ to $t = t$ and $q_t = 0$ to $q_t = q_t$; this equation can be written as the following linear form :

$$t/q_t = 1/k_2q_e^2 + t/q_e \quad (7)$$

where K_2 (g/mg.h) is the rate constant for the pseudo-second order rate expression. The plots of t/q_t versus t at 310 K for different compositions of hydroxyapatites of Ca/P=1.50, 1.54, 1.58, 1.62 and 1.67 are given in **Fig. 7**. The values of the amount adsorbed at equilibrium q_e (mg/g) according to pseudo-second order model and the values of K_2 are determined from the slopes and intercepts of the linear plots, respectively and are shown in **Table 4**.

The initial rate of adsorption g (mg/g.h), is also calculated by using the relation as follows;

$$g = K_2q_e^2 \quad (8)$$

The values obtained of g (**Table 4**), indicate that all hydroxyapatites studied of Ca/P ratio between 1.50 and 1.67 have the same initial rate of adsorption reaction, these values are between 166 and 170 mg/g.h.

The experimental q_e (exp) and calculated q_e (cal) values of the maximum amount adsorbed are almost equal to each adsorbent, and the high values of the correlation coefficient ($R^2 > 0.99$) which are close to unity, indicate that pseudo-second order model is suitable to explain the reaction mechanisms for the methionine adsorption by these five hydroxyapatites.

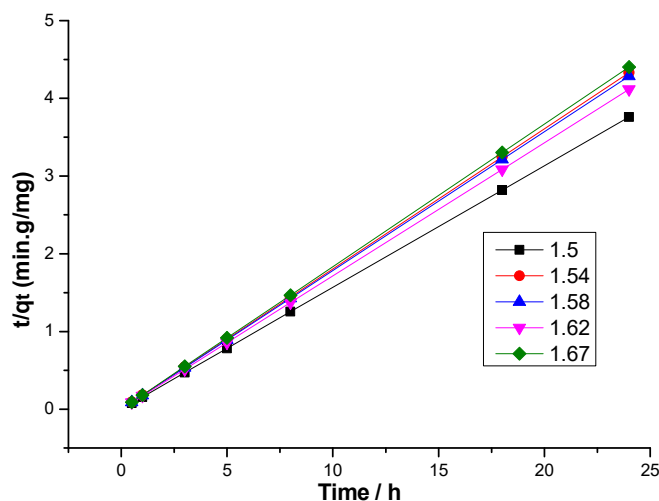


Fig. 7. Pseudo-second-order kinetics for adsorption of methionine on hydroxyapatites of Ca/P between 1.50 and 1.67

Elovich kinetic model. This model is used to verify and describe chemisorption. The following form of Elovich equation was applied, as suggested by Chien and Clayton ;²⁷

$$dq_t / dt = \alpha \exp(-\beta q_t) \quad (9)$$

Integrating and applying the limits for $t(0, t)$ and $q_t (0, q_t)$, the Elovich model can be linearized as;

$$q_t = \ln(\alpha.\beta) / \beta + \ln t / \beta \quad (10)$$

where q_t is the amount adsorbed at time t (h), α (mg/g.h) is the initial adsorption rate and β (g/mg) is the desorption constant during the adsorption process. The β and α constants are calculated, respectively, from the slope and intercept of the linearized plot of q_t versus $\ln t$ (**Fig.8**) and are summarized in **Table 4**. We have noted that α and β varied as a function of Ca/P of hydroxyapatite, they increased when Ca/P increased from 1.50 to 1.67. The regression coefficients R^2 from the simulated data is between 0.84 and 0.95. The values of α , β and R^2 mean that the adsorption rate of this model could be part of the rate limiting step, and the desorption constant increases from hydroxyapatite containing more of HPO_4^{2-} (Ca/P=1.50) to hydroxyapatite exempt of these ions (Ca/P=1.67), this probably suggests a type of chemisorption confirmed by kinetic model of pseudo second-order, but in overall, the Elovich model could not simulate the experimental data perfectly well.

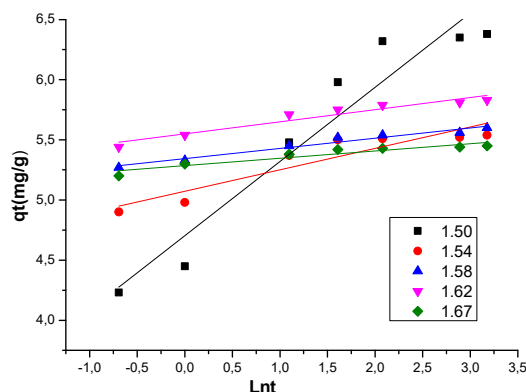


Fig. 8. Plot of Elovich equation for adsorption of methionine on hydroxyapatites of Ca/P between 1.50 and 1.67

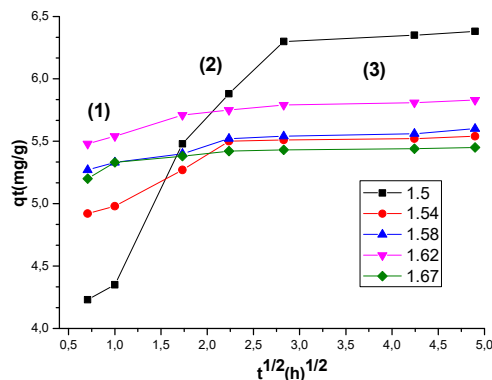
Intraparticle diffusion model. This model proposed by Weber and Morris was applied to the kinetic data with the pore diffusion factor defined by the following equation :²⁸

$$q_t = K_p t^{1/2} + C \quad (11)$$

where, q_t is the amount of methionine adsorbed at time t (h), K_p ($mg \cdot g^{-1} \cdot h^{0.5}$) is the rate constant for intraparticle diffusion model and the intercept (C) is a constant indicative of the boundary layer thickness effect. The K_p and C constants are calculated from the plot of q_t versus $t^{1/2}$ (**Fig. 9**) and given in **Table 4**. The rate constant K_p is influenced by the composition of hydroxyapatite, its decreases from 0.516 to 0.045 $mg \cdot g^{-1} \cdot h^{0.5}$ when the Ca/p increases from 1.50 to 1.67 while the C constant is not zero, and it increases when the Ca/P increases. This result indicates that the rate of adsorption is important for apatite containing more HPO_4^{2-} ions. The regression coefficient values R^2 obtained from curves in **Fig. 9** are not satisfactory, they are between 0.614 and 0.809 (**Table 4**), which indicates that intra-particle diffusion may not be the controlling factor in determining the kinetics of the process. The plots of q_t versus $t^{1/2}$ have shown multi-linearity with three different adsorption stages (1), (2) and (3); portion (1) is between 0.5 and 3 hours, portion (2) is between 3 and 8 hours and the portion (3) is between 8 and 24 hours (**Fig. 9**). **Table 5** shows that the intraparticle diffusion rate constants, K_p , decrease and the C constants increase when going from range (1) to range (3) for all the apatites studied. The calculated values of the regression coefficient, R^2 , for all portions (**Table 5**) show the difficulty of finding the most limiting step to control and determine the intraparticle diffusion rate. Therefore, the intraparticle diffusion adsorption mechanism appeared complex for all these apatites.

Table 5. Parameters for intraparticle diffusion model in three adsorption stages: (1) for [0.5-3h], (2) for [3-8h] and (3) for [8-24h] for all the apatites studied.

	1.50			1.54			1.58			1.62			1.67		
	K_p	C	R^2	K_p	C	R^2	K_p	C	R^2	K_p	C	R^2	K_p	C	R^2
(1)	1.281	3.217	0.925	0.352	4.653	0.971	0.121	5.195	0.922	0.226	5.317	0.998	0.151	5.125	0.551
(2)	0.747	4.194	0.998	0.213	4.943	0.483	0.125	5.203	0.641	0.072	5.585	0.996	0.044	5.308	0.725
(3)	0.038	6.191	0.991	0.013	5.470	0.698	0.026	5.460	0.698	0.018	5.736	0.914	0.009	5.403	0.914



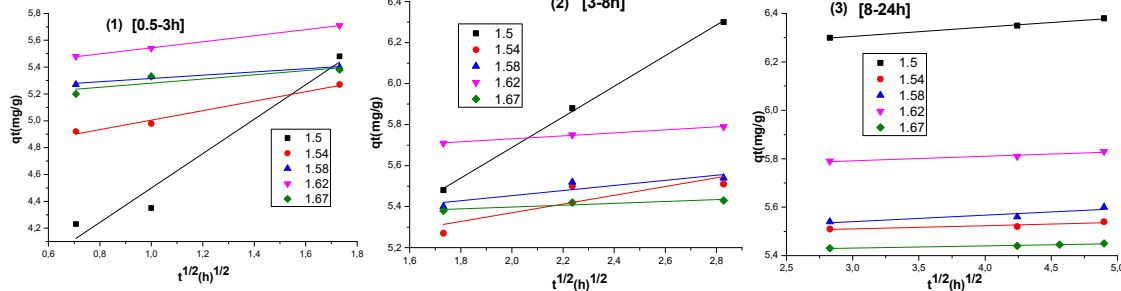


Fig. 9. Intra-particle diffusion model plot for adsorption of methionine on hydroxyapatites of Ca/P between 1.50 and 1.67 : (1) for [0.5-3h], (2) for [3-8h] and (3) for [8-24h]

Table 4. Parameters for various kinetic models for methionine adsorption on hydroxyapatites of Ca/P between 1.50 and 1.67 at 310 K, initial methionine concentration 149.2 mg/L, pH \sim 7 and adsorbent dose 20 mg.

Kinetic models	Parameters	Hydroxyapatites				
		1.50	1.54	1.58	1.62	1.67
Pseudo-first order	$K_1 (h^{-1})$	0.252	0.201	0.430	0.156	0.179
	$q_e (cal) (mg/g)$	1,874	0.386	0.431	0.229	0.150
	$q_e (exp) (mg/g)$	6.380	5.540	5.610	5.720	5.440
	$R^2 (\%)$	0.899	0.713	0.714	0.878	0.736
Pseudo-second order	$K_2 (g/mg, h)$	4.081	5.522	5.280	4.927	5.581
	$q_e (cal) (mg/g)$	6.382	5.555	5.618	5.831	5.464
	$q_e (exp) (mg/g)$	6.390	5.540	5.610	5.720	5.440
	$g (mg/g, h)$	166.07	170.03	166.76	167.23	166.35
	$R^2 (\%)$	0.9997	0.9998	0.9998	0.9998	0.9999
Elovich	$\beta (g/mg)$	1.623	5.618	11.765	10.000	16.470
	$\alpha (mg/g, h)$	$1.27 \cdot 10^3$	$4.24 \cdot 10^{11}$	$1.71 \cdot 10^{26}$	$1.27 \cdot 10^{23}$	$3.92 \cdot 10^{36}$
	$R^2 (\%)$	0.913	0.840	0.960	0.918	0.864
Intra-particle diffusion	$K_p (mg, g^{-1}, h^{0.5})$	0.516	0.144	0.074	0.076	0.045
	$C (mg/g)$	4.264	4.958	5.275	5.509	5.265
	$R^2 (\%)$	0.728	0.654	0.809	0.724	0.614

Among all the four kinetics models applied to the experimental data, the pseudo-second-order model is the best-fitted model with the higher R^2 values ($R^2 > 0.99$) and a good correlation between the theoretical and experimental q_e values. However, we found that the adsorption process of methionine by hydroxyapatites of Ca/P between 1.50 and 1.67 also involved the Elovich kinetic model and intraparticle diffusion, indicating a complex adsorption mechanism.

3.1.2 Adsorption isotherms

Adsorption equilibrium is a fundamental property in adsorption studies. Adsorption isotherms are very important in order to design adsorption processes; they also provide the adsorption capacity of the adsorbent under a given set of conditions. Therefore, adsorption data were adjusted to four isotherm models : Langmuir,²⁹ Freundlich,³⁰ Temkin,³¹ and Dubinin-Raduskevich³². The evolution of the amounts of methionine adsorbed $q_e (mg/g)$ on hydroxyapatites of Ca/P between 1.50 and 1.67 versus its equilibrium concentration $C_e (mg/L)$, at the initial pH \sim 7 and at 310 K, are represented in **Fig.10**.

The quantity adsorbed increases quickly as the equilibrium methionine concentration increases, this means that the hydroxyapatites studied could adsorb significant quantities of methionine.

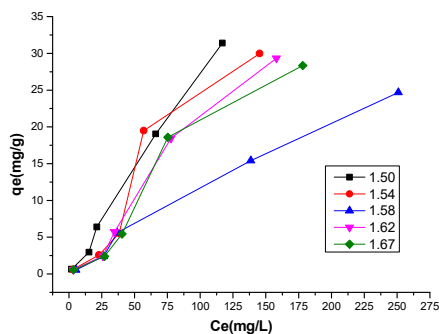


Fig. 10. Adsorption isotherms of methionine on hydroxyapatites of Ca/P between 1.50 and 1.67 (solid quantity : 20 mg, stirring time : 1 min, T : 310 K)

Langmuir isotherm. This isotherm is defined by the following equation :

$$q_e = q_m K_L C_e / (1 + K_L C_e) \quad (12)$$

The linear form of this expression is given by equation:

$$1/q_e = 1/q_m + 1/K_L q_m C_e \quad (13)$$

where C_e (mg/L) is the equilibrium concentration of the methionine, q_e (mg/g) is the amount of adsorbate per unit mass of hydroxyapatite, K_L (L/g) and q_m (mg/g) are the Langmuir constants related to free interaction binding energies of the adsorption capacity and the maximum adsorption capacity, respectively. From the straight lines adjusted to graphs $1/q_e$ versus $1/C_e$ (Fig. 11), the q_m and K_L values are calculated from the intercept and the slope, respectively, for five isothermal lines and they are presented in Table 6. It was observed that the maximum adsorption capacity corresponding to complete monolayer coverage of hydroxyapatite with methionine was found to be between 20.83 and 25.57 mg/g and the adsorption coefficient, K_L , value decreased from 15.98 to 7.26 L/g as the Ca/P of hydroxyapatite increased from 1.50 to 1.67. Therefore, the interaction between adsorbate and adsorbent is very important for hydroxyapatite of Ca/P=1.50, which contains the most HPO_4^{2-} ions. The result of high correlation coefficient values ($R^2 > 0.98$) showed a good fit to the experimental data.

In order to assess the favorability and effectiveness of the Langmuir adsorption process, the dimensionless separation parameter noted R_L can be determined by the following equation :³³

$$R_L = 1 / (1 + K_L C_0) \quad (14)$$

where K_L is the Langmuir constant (l/g) and C_0 is the initial methionine concentration (mg/L). The value of R_L indicates the type of the isotherm to be either irreversible ($R_L = 0$), linear ($R_L = 1$), favorable ($0 < R_L < 1$) or unfavorable ($R_L > 1$). Fig. 12 represents the evolution of the estimated value of R_L as a function of the initial concentration of methionine in the aqueous solution for different compositions of hydroxyapatite. the R_L values obtained are between 0 and 1, indicating that the Langmuir isotherm is favorable for the adsorption of methionine on hydroxyapatite at physiological temperature.

From the Langmuir constant K_L that is related to free interaction binding energies of the adsorption capacity, it is possible to prove the nature of the adsorption process by calculating the free energy thermodynamic parameter ΔG_{ads}^0 (J/mol) of adsorption by the following equation :³⁴

$$\Delta G_{ads}^0 = -R T \ln K_L \quad (15)$$

where R (8.314 J mol⁻¹ K⁻¹) is the universal gas constant and T is the absolute temperature in Kelvin. The values of ΔG^0 found at 310 K for different hydroxyapatites (Table 5) are between -4.43 and -7.14 KJ/mol, they are negative and between -20 KJ/mol and 0 KJ/mol, revealing that the adsorption is a spontaneous process, exothermic and is often as physical type.³⁵

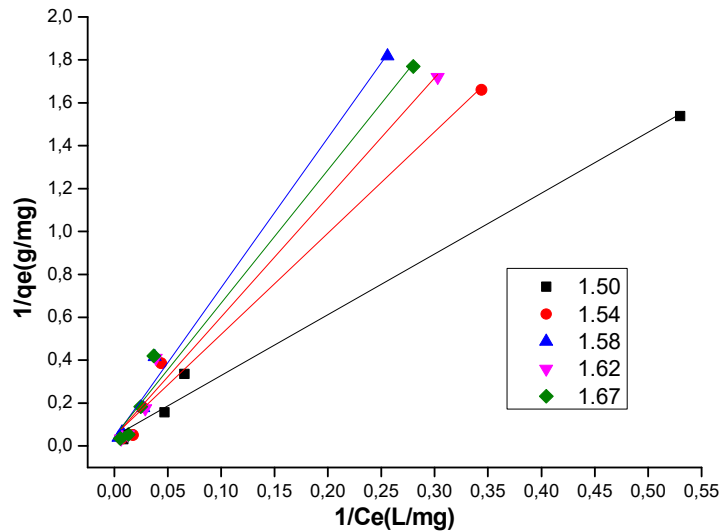


Fig. 11. Langmuir isotherm model

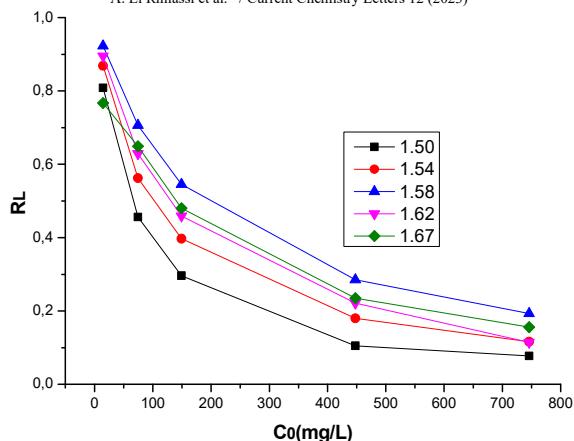


Fig. 12. Evolution of dimensionless separation factor values R_L for methionine adsorption by hydroxyapatites of Ca/P between 1.50 and 1.67 at 310 K

Freundlich isotherm. This empirical model can be described by the equation:

$$q_e = K_F C_e^{\frac{1}{n}} \quad (16)$$

The linear form of this equation is given by the following form:

$$\ln(q_e) = \ln(K_F) + \frac{1}{n} \ln(C_e) \quad (17)$$

where C_e (mg/L) is the equilibrium concentration of methionine in the bulk solution, q_e (mg/g) is the amount of solute adsorbed per unit weight of adsorbent, K_F (L/mg) is a Freundlich constant relative to the adsorption capacity of the adsorbent and $1/n$ is the heterogeneity factor relative to the adsorption intensity, which indicates the adsorption process to be either favorable ($0.1 < 1/n < 1$) or poor ($1/n > 1$). Plotting $\ln q_e$ versus $\ln C_e$ results in a straight line of intercept $\ln K_F$ and slope $1/n$ (Fig. 13). The values of K_F , $1/n$ and R^2 the regression coefficients are presented in Table 6. We find that K_F depends on the composition of the hydroxyapatite, it decreases from 0.395 to 0.110 L/mg when Ca/P increases from 1.50 to 1.67, it is the same remark as for the Langmuir constant K_L . The R^2 values corresponding to all apatites are between 0.91 and 0.99, showing that this model is not as good as Langmuir's isothermal model in describing the experimental data. It is observed that the values of $1/n$ are found less than or equal to one ($1/n \leq 1$), indicating that the adsorption processes tend to be favorable.

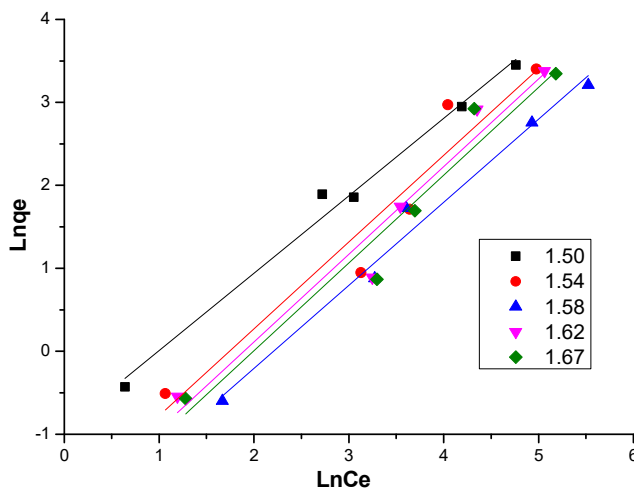


Fig. 13. Freundlich isotherm model

Temkin isotherm. This isotherm can be described by the following equation:

$$q_e = (R T / b_t) \ln (a_t C_e) \quad (18)$$

This equation can be expressed in its linear form as :

$$q_e = (R T/b_t) \ln a_t + (R T/b_t) \ln C_e \quad (19)$$

where q_e (mg/g) and C_e (mg/L) are the amount of adsorbate per unit mass of adsorbent and the equilibrium concentration of adsorbate, respectively. b_t (KJ/mol) and a_t (L/mg) are the Temkin isotherm constants associated with the heat of adsorption and the maximum binding energy, respectively. T (310K) and R (8.314 Jmol⁻¹K⁻¹) are the temperature and the universal gas constant, respectively. Plotting q_e versus $\ln C_e$ results in a straight line of intercept $(R T/b_t) \ln a_t$ and slope $R T/b_t$ (Fig. 14). The values of R^2 , regression coefficients and the constants are presented in Table 6. The R^2 values of the Temkin model are between 0.90 and 0.99, they are almost equal to the values of the Freundlich model but they are lower than those of the Langmuir model, suggesting that Temkin's model can satisfy the experimental data and similar results was obtained in the interaction of insulin with synthetic hydroxyapatite.⁵ We find that the Temkin constant a_t depends on the composition of the hydroxyapatite, it decreases from 0.077 to 0.042 L/mg when Ca/P increases from 1.50 to 1.67, it is the same remark as for the Langmuir constant K_L and Frundlich constant K_F . It is interesting to noted that the values of b_t obtained for all hydroxyapatites are between 0.163 and 0.277 KJ/mol . They are weak and positive, indicating that the adsorption processes are exothermic and can be considered purely electrostatic.

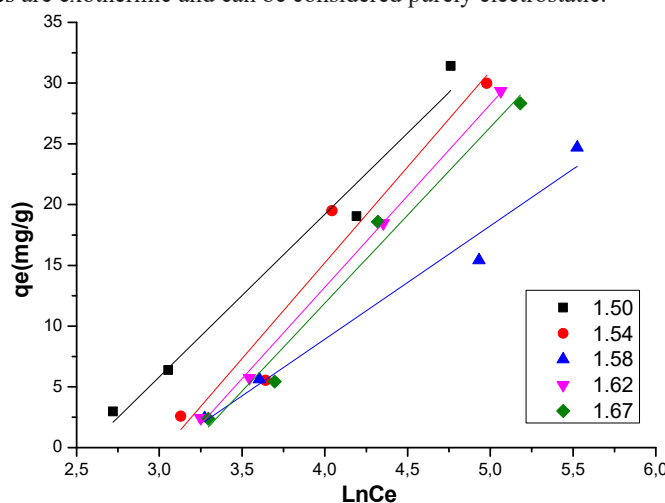


Fig. 14. Temkin isotherm model

Dubinin–Kaganer–Radushkevich isotherm. This model can be represented by the empirical equation below:

$$q_e = q_D \exp(-B_D \mathcal{E}^2) \quad (20)$$

The linearized form of this equation is given as follows:

$$\ln q_e = \ln q_D - B_D \mathcal{E}^2 \quad (21)$$

with

$$\mathcal{E} = R T \ln(1 + 1/C_e) \quad (22)$$

$$E = 1/\sqrt{2 B_D} \quad (23)$$

where q_e (mg/g) is the amount of methionine per unit mass of hydroxyapatite used, q_D (mg/g) is the maximum adsorption capacity, B_D (mol/kJ)² is the model constant related to mean adsorption free energy E (J/mol), \mathcal{E} (mol/kJ)² is the Polanyi potential, R (8.314 JK⁻¹mol⁻¹) is the universal gas constant, T (k) is the adsorption temperature. The plot of $\ln q_e$ against \mathcal{E}^2 (Fig.15) gives the slope and intercept as B_D and q_D , respectively (Table 6). The adsorption energy E obtained decreased from about 95 to 42 J/mol when the Ca/P atomic ratio increased from 1.50 for the hydroxyapatite containing the maximum of HPO₄²⁻ ions to 1.67 for the stoichiometric hydroxyapatite. This energy is less than 8 KJ/mol, indicating that the adsorption of methionine on hydroxyapatites can be attributed to the physical mechanisms of adsorption at 310 K, which is in agreement with the above study. The q_D value found is between 20.2 and 28.1 mg/g and is important for hydroxyapatite of Ca/P=1.50. The values of the regression coefficient found are between 0.80 and 0.97, they are lower than the values corresponding to Temkin, Freundlich, and Langmuir models, which means that the D-R model does not simulate the data experimental well.

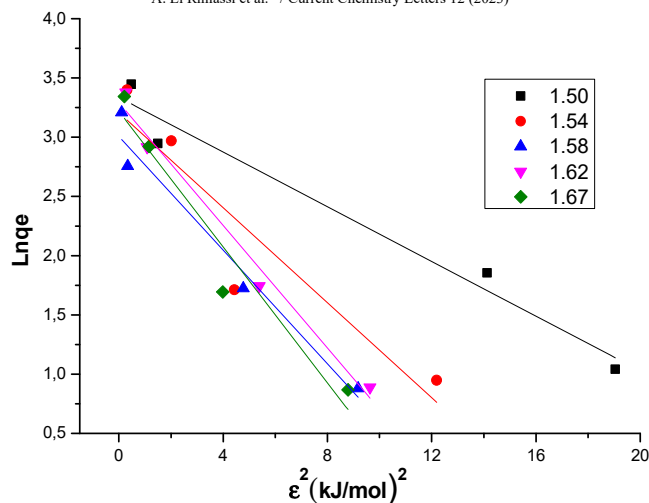


Fig.15. Dubinin–Kaganer–Radushkevich isotherm model

Table 6. Values of the parameters of Langmuir, Freundlich, Temkin and Dubinin–Kaganer–Radushkevich models for the adsorption of methionine on hydroxyapatites of Ca/P between 1.50 and 1.67 at 310 K.

Models	Parameters	Hydroxyapatites				
		1.50	1.54	1.58	1.62	1.67
Langmuir	$K_L(L/g)$	15.981	10.172	5.593	7.892	7.261
	$q_m(mg/g)$	22.075	20.830	25.575	22.727	22.187
	$R^2(\%)$	0.988	0.982	0.990	0.980	0.982
	$\Delta G_{ads}^0(KJ/mol)$	-7.143	-5.978	-4.435	-5.324	-5.109
Freundlich	$K_F(L/mg)$	0.395	0.162	0.110	0.135	0.121
	$1/n$	0.933	1.045	1.001	1.057	1.058
	n	1.072	0.956	0.998	0.946	0.945
	$R^2(\%)$	0.985	0.908	0.977	0.942	0.931
Temkin	$b_t(KJ/mol)$	0.193	0.163	0.277	0.171	0.178
	$a_t(L/mg)$	0.077	0.048	0.047	0.044	0.042
	$R^2(\%)$	0.963	0.904	0.964	0.998	0.988
	Dubinin–Kaganer–Radushkevich (D-K-R)	$E(KJ/mol)$	95.347	49.925	45.739	44.020
$B_D(mol/kJ)^2$		0.116	0.201	0.239	0.258	0.286
$q_D(mg/g)$		28.106	24.727	20.201	26.894	25.013
$R^2(\%)$		0.954	0.806	0.952	0.975	0.919

Compared to, Freundlich, Temkin, and Dubinin-Radushkevich models, the Langmuir model appears to be the most appropriate isotherm for the fit of the equilibrium experimental data of adsorption of methionine on the hydroxyapatites of Ca/P between 1.50 and 1.67 under concentration range studied and at 310K. Indeed, the values of R^2 for the Langmuir adsorption isotherm are close to 1, they are larger than those of the Freundlich, Temkin and Dubinin–Kaganer–Radushkevich (D-K-R) adsorption isotherms. The dominance of the Langmuir model quantitatively describes the formation of a monolayer of methionine on the outer surface of the hydroxyapatite.

3.2 Study of the solids

Fig. 16 and **Fig. 17** present the infrared spectrums of different hydroxyapatites with an atomic ratio Ca/P = 1.50, 1.54, 1.58, 1.62 and 1.67 after adsorption in 149.2 mg/g of the amino acid methionine in 18 h of contact time. In addition to the bands associated with the PO_4^{3-} and HPO_4^{2-} ions of the hydroxyapatite, these spectra reveal the presence of bands characteristic of methionine. Indeed, the bands attributable to C=O appear at 1641 and 1730 cm^{-1} due to the carboxyl group $-COO^-$ of the amino acid.³⁶ Other low-intensity bands appear between 1481 and 1550 cm^{-1} which may be due to the NH_2 or NH_3^+ groups of methionine attached to the surface of the apatites.³⁶ The band observed at 1340 cm^{-1} is due to the vibration of the C-H bond attributable to the CH group of amino acids.³⁶ All of these FT-IR spectroscopy results confirm the adsorption of the amino acid used.

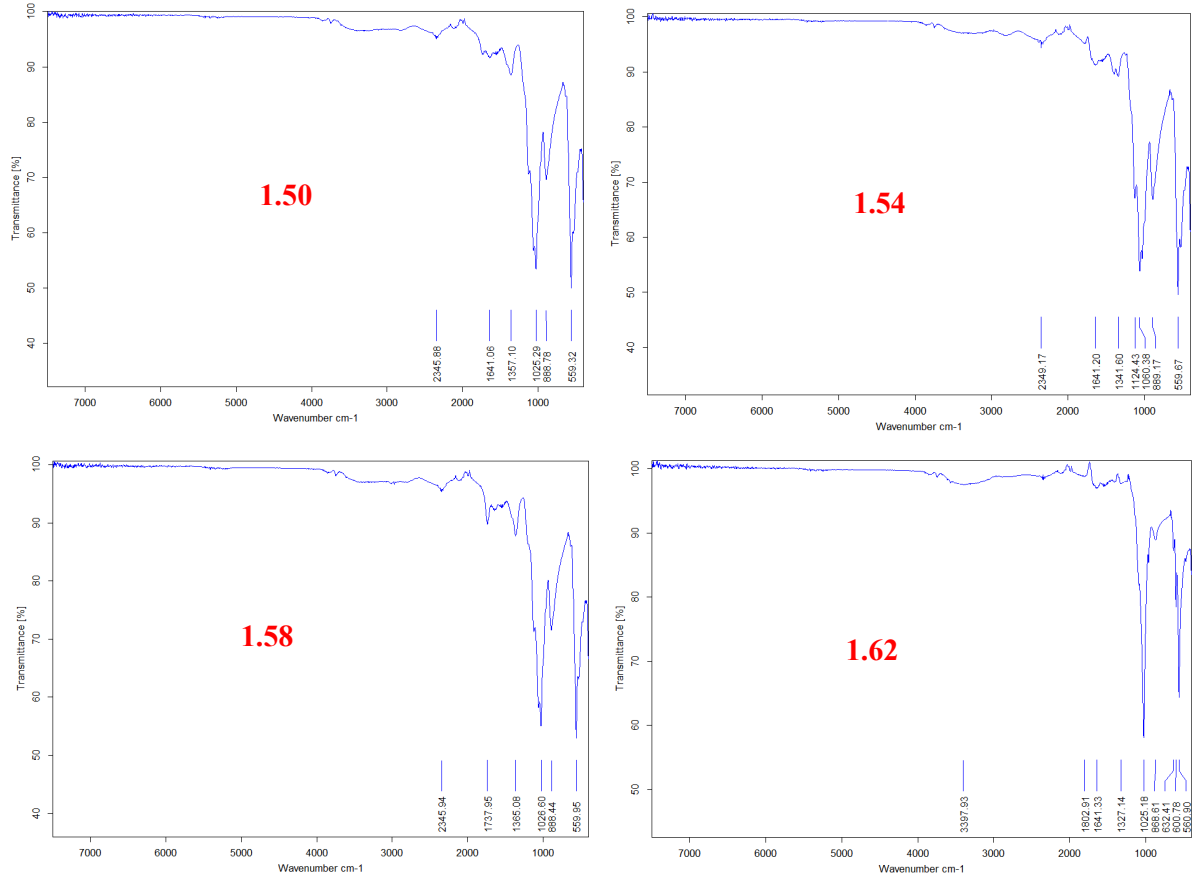


Fig. 16. FTIR spectra of non-stoichiometric hydroxyapatites of Ca/P between 1.50 and 1.62 after adsorption in 149.2 mg/g of methionine

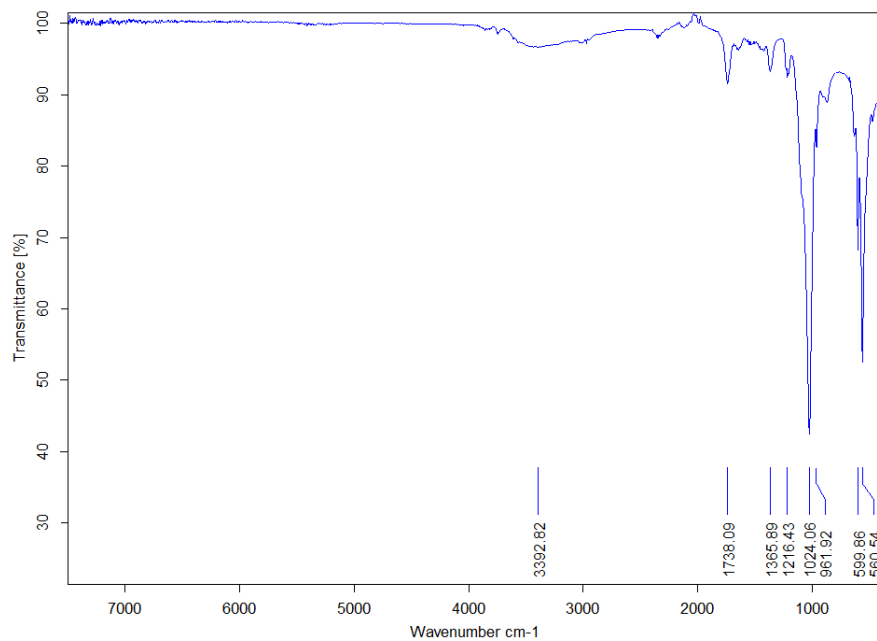


Fig. 17. FTIR spectra of stoichiometric hydroxyapatite of Ca/P=1.67 after adsorption in 149.2 mg/g of methionine

3.3 Temperature effect and thermodynamic parameters

In the present work, the influence of temperature on the adsorption process of methionine on hydroxyapatites was studied in an interval between 298 and 318 k. The results obtained from the variation of the amount adsorbed as a function of the temperature for 18 hours and for initial concentration $C_0=149.2$ mg/L of amino acid are represented in **Fig. 18**. The increase in temperature causes a slight decrease in the quantity adsorbed at equilibrium $q_e(\text{mg/g})$ of amino acid, which is in agreement with the results of previous work.⁴

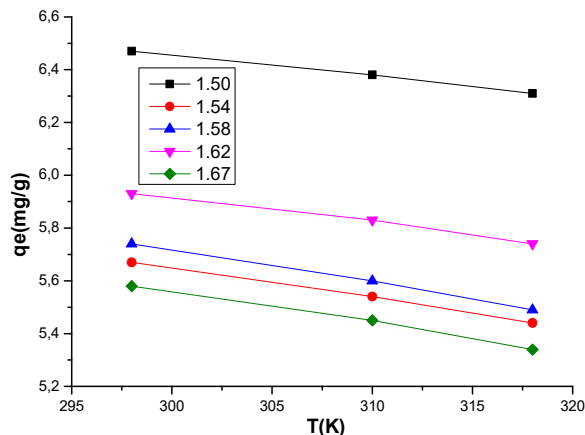


Fig. 18. Evolution of the adsorbed amount of methionine on hydroxyapatites of Ca/P between 1.50 and 1.67 as a function of temperature

In order to verify and determine the nature and spontaneity of adsorption processes, thermodynamic parameters such as ΔG , ΔH and ΔS in solution were calculated using the following standard thermodynamic relations :^{37,38}

$$K_C = (C_0 - C_e)/C_e \quad (24)$$

$$\Delta G = -RT \ln K_C \quad (25)$$

$$\Delta G = \Delta H - T\Delta S \quad (26)$$

where K_C is the thermodynamic equilibrium constant, C_0 and $C_e(\text{mg/L})$ are respectively the initial and equilibrium concentration of the methionine in solution, $\Delta G(\text{J/mol})$ is the change in Gibbs free energy, $\Delta H(\text{J/mol})$ is the change in enthalpy, $\Delta S(\text{J/mol})$ is the change in entropy, T is the temperature in Kelvin and R is the universal gas constant ($8.314 \text{ J mol}^{-1} \text{ K}^{-1}$). The values of K_C are calculated from relation (24), ΔG parameter is calculated at different temperatures (298k, 310k and 318k) from relation (25), and ΔH and ΔS parameters are determined respectively, from the intercept and slope of a plot of ΔG against T (**Fig. 19**). The values of all parameters are presented in **Table 7**.

The negative values of ΔG indicate the spontaneous nature of the adsorption of the methionine on hydroxyapatites of Ca/P between 1.50 and 1.67. The ΔG values decrease weakly with increasing temperature indicating that the adsorption process is unfavorable at high temperatures. Moreover, the values of ΔG are between -20 and 0 kJ/mol confirming that the adsorption processes of methionine on hydroxyapatites can be physical adsorption.³⁹ The negative value of ΔH showed that the adsorption process is exothermic in nature, the low values of this parameter suggest that the adsorption process can be pure physisorption.⁴⁰ This agrees with the values of the parameters obtained from the quantities ΔG_{ads}^0 of Langmuir and b_t of Temkin. The negative values of ΔS revealed an in-order at the solid/solution interface of the methionine molecules towards the surface of hydroxyapatite during the adsorption process.

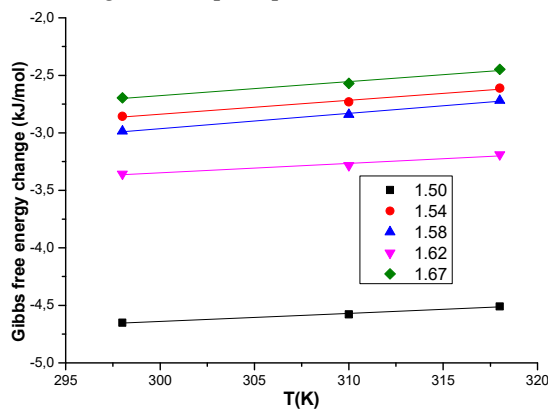


Fig. 19. Van't Hoff plot

Table 7. Thermodynamic parameters for methionine adsorption onto the hydroxyapatites of Ca/P between 1.50 and 1.67.

Parameters	T(k)	1.50	1.54	1.58	1.62	1.67
$\Delta G(kJ/mol)$	298	-4.651	-2.857	-2.986	-3.357	-2.695
	310	-4.578	-2.731	-2.841	-3.284	-2.570
	318	-4.509	-2.612	-2.719	-3.189	-2.448
$\Delta H(kJ/mol)$		-6.746	-6.472	-6.938	-5.813	-6.336
$\Delta S(J/mol\ k)$		-7.022	-12.106	-13.228	-8.165	-12.176
$R^2(\%)$		0.998	0.993	0.997	0.985	0.991

4. Conclusion

The apatites used in this work are prepared by co-precipitation at 298k and at pH~7.4. The results obtained from chemical analysis and characterization techniques indicate that these apatites have a Ca/P ratio of between 1.50 and 1.67; they are of low crystallinity. Indeed, the apatites of Ca/P=1.50, 1.54, 1.58 and 1.62 are non-stoichiometric hydroxyapatites and the apatite of Ca/P=1.67 is called stoichiometric hydroxyapatite.

In this paper, we are interested to study the adsorption capacity of L-methionine, an essential amino acid that contains sulfur and has a character hydrophobic, on hydroxyapatite with Ca/P ratios between 1.50 and 1.67. The results of our investigation focused on the influence of the chemical composition of the hydroxyapatite used on the specific parameters of the adsorption process such as the incubation time, the initial methionine concentration and the effect of temperature. The results found are collected, analyzed and interpreted. The adsorption kinetics are relatively fast and equilibrium was reached after the first hours of contact, testing the high reactivity of poorly crystalline hydroxyapatites toward the L-methionine presenting various functional groups. The adsorption process is influenced by the composition of the hydroxyapatite in HPO_4^{2-} ions. Indeed, the high amounts adsorbed at saturation are obtained for the compounds, non-stoichiometric, containing more HPO_4^{2-} ions and having a high specific surface area.

The pH of the incubation medium of the adsorption reaction is between 6 and 7, it is higher than that of the isoelectric point (PI=5.74) of methionine and approximately equal to the point of zero charge (pH_{pzc}) of hydroxyapatites, which shows that the methionine molecules are negatively charged ($CH_3S(CH_2)_2CH(NH_2)COO^-$), while the apatites surfaces used are negatively charged or maybe have the equality between the positive charges and the negative charges. In this case, an ionic exchange or attraction mechanism is established between the ions of the surface of the apatites and the methionine charge. Therefore, the interaction between methionine and hydroxyapatites is considered electrostatic interaction.

Modeling of adsorption kinetics shows that the adsorption mechanism is perfectly described by pseudo-second-order kinetics. Indeed, the regression coefficients are very close to unity ($R^2 > 0.999$) and the values of experimental and calculated maximum adsorption capacities are almost the same, indicating that the interactions between group functionals of methionine and hydroxyapatites may be governed by ionic bindings.

Modeling of adsorption isotherms shows that Langmuir's model gives a better fit of experimental data compared to that of Freundlich, Temkin and Dubinin-Kaganer-Radushkevich, suggesting that the energetic properties of hydroxyapatites adsorption sites are uniform with one molecule of methionine per site, which assumes that a monolayer of methionine is formed. The detailed study of the parameters related to these models can reveal that the adsorption process is spontaneous, favorable, and often controlled by physisorption.

The results of the Fourier transform infrared spectroscopy after adsorption prove the existence of new bands which did not exist before adsorption, which confirms the fixation of methionine on the adsorbents. Furthermore, the position of the bands observed in the 1400-1730 cm^{-1} range and their intensities suggest the cationic form of methionine attached to hydroxyapatite. Indeed, the presence of bands characteristic of the carboxyl groups $-COO^-$ and the absence of bands attributed to the $-COOH$ groups (1600 cm^{-1}), indicate that the adsorption is mainly due to the electrostatic interaction between the $-COO^-$ groups methionine and calcium Ca^{2+} hydroxyapatite ions.

The thermodynamic study shows that the methionine adsorption process on the different forms of hydroxyapatite is considered spontaneous ($\Delta G^0 < 0$), and exothermic ($\Delta H < 0$) and may be of a physical nature with interactions mainly electrostatic.

The study of isotherms, kinetics and thermodynamics of the adsorption of L-Methionine on poorly crystalline hydroxyapatite with different Ca/P ratios can help to understand the properties of the interaction of biomolecules such as proteins, peptides, antibodies, or drugs, with biological apatites used in several applications and especially in the biomedical field.

This work can be considered clear evidence that proves the importance of applied chemistry in various fields, as previously reported in multiple scientific papers.

Acknowledgements

The authors acknowledge members of the laboratory of the chemistry department of the Faculty of Sciences, Ibn Tofail University to support this study.

References

- 1 El Rhilassi A., Mourabet M., El Boujaady H., Bennani-Ziatni M., El Hamri R., and Taitai A. (2012) Adsorption and release of amino acids mixture onto apatitic calcium phosphates analogous to bone mineral. *Appl. Surf. Sci.*, 259, 376–384.
- 2 El Rhilassi A., Mourabet M., Bennani-Ziatni M., El Hamri R., and Taitai A. (2016) Interaction of some essential amino acids with synthesized poorly crystalline hydroxyapatite. *J. Saudi Chem. Soc.*, 20, S632–S640.
- 3 El Rhilassi A. and Bennani-Ziatni M. (2022) Experimental study on the interaction of insulin with apatitic calcium phosphates analogous to bone mineral : adsorption and release. *Curr. Chem. Lett.*, 11, 341–352.
- 4 El Rhilassi A., Mourabet M., El Boujaady H., Bennani Ziatni M., El Hamri R., and Taitai A. (2014) Adsorption of some essential amino acids and their mixture onto poorly crystalline hydroxyapatite. *J. Mater. Environ. Sci.*, 5 (5) 1442–1453.
- 5 El Rhilassi A., and Bennani Ziatni B. (2023) Studies of kinetic models and adsorption isotherms : application on the interaction of insulin with synthetic hydroxyapatite. *Curr. Chem. Lett.*, 12, 445–458.
- 6 Pon-On W., Charoenphandhu N., Tang I. M., Jongwattapanisan P., Krishnamra N., and Hoonsawat R. (2011) Encapsulation of magnetic CoFe₂O₄ in SiO₂ nanocomposites using hydroxyapatite as templates : A drug delivery system. *Mater. Chem. Phys.*, 131 (1–2) 485–494.
- 7 Zhang C., Li C., Huang S., Hou Z., Cheng Z., Yang P., Peng C., and Lin J. (2010) Self- activated luminescent and mesoporous strontium hydroxyapatite nanorods for drug delivery. *Biomaterials*, 31 (12) 3374–3383.
- 8 Rey C. (1998) Calcium phosphates for medical applications. In : Amjad Z editor. Calcium phosphates in biological and industrial systems. *Boston : Kluwer Academic Publishers*, 217–39.
- 9 Winand L. (1961) Etude physico-chimique du phosphate tricalcique hydrate et de l'hydroxyapatite. *Annali di Chimica*. 6, 941–967.
- 10 Lin J.H.C., Kuo K.H., Ding S.J., and Ju C. P. (2001) Surface reaction of stoichiometric and calcium-deficient Hydroxyapatite in simulated body fluid. *J Mater Sci Mater Med.*, 12 (8) 731–741.
- 11 Li H., Gong M., Yang A., Ma J., Li X., and Yan Y. (2012) Degradable biocomposite of nano calcium deficient hydroxyapatite-multi (amino acid) copolymer. *Int. J. Nanomed.*, 7, 1287–1295.
- 12 Suzuki O., Kamakura S., Katagiri T., Nakamura M., Zhao B., Honda Y., Kamijo R. (2006) Bone formation enhanced by implanted octacalcium phosphate involving conversion into Ca-deficient hydroxyapatite. *Biomater.*, 27, 2671–2681.
- 13 Dorozhkin S.V. (2002) A review on the dissolution models of calcium apatites. *Prog Cryst Growth Charact.*, 44 (1) 45–61.
- 14 Rey, C., Hina, A., Tofighi, A., Glimcher, M.J. (1995) Maturation of poorly crystalline apatites : Chemical and structural aspects in vivo and in vitro. *Cells Mater.*, 4–5, 345–356.
- 15 Dawson R.M.C., Elliott D.C., Elliott W.H., and Jones K.M., eds. (1969) *Data for Biochemical Research*, Oxford University Press., 436–465.
- 16 Weast., and Robert C., ed. (1981) *CRC Handbook of Chemistry and Physics* (62nd ed.). Boca Raton, FL : *CRC Press.*, C-374.
- 17 Pavia D. L., Lampman G. M., Kriz G. S., and Vyvyan, J. R. (2015) *Introduction to Spectroscopy*, 5th edition; Cengage Learning: Stamford, CT, ISBN-13: 978-1-285-46013-0.
- 18 Silverstein R. M., and Webster F. X. (1997) *Spectrometric Identification of Organic Compounds*, 6th Edn, *John Wiley and Sons, Hoboken*, 12-20.
- 19 Sears G.W. (1956) Determination of specific surface area of Colloidal silica by titration with sodium hydroxide, *Anal. Chem.*, 28 (12) 1981 – 1983.
- 20 Noh J. S., and Schwarz J. A. (1989) Estimation of the point of zero charge of simple oxides by mass titration. *J. Colloid Int Sci.*, 130 (1) 157–164.
- 21 Rey C. and Hina A. (1995) Surface reactivity of bone mineral crystals, a model for bioactive orthopaedic materials, *bioceramics*, 8, 55–60.
- 22 Destainville A., Champion E., and Bernache-Assollante D. (2003) Synthesis, characterization and thermal behaviour of apatite tricalcium phosphate, *Mater. Chem. Phys.*, 80, 269 – 277.
- 23 Raynaud S., Champion E., Bernache-Assollant D., and Thomas P. (2002) Calcium phosphate apatite with variable Ca/P atomic ratio I. Synthesis, characterisation and thermal stability of powders. *Biomaterials*, 23(4)1065-72.
- 24 Kwon S.H., Jun Y.K., Hong S.H., and Kim H. E. (2003) Synthesis and dissolution behaviour of β - TCP and HA/ β - TCP composite powders. *J. Eur. Ceram. Soc.*, 23 (7) 1039-1045.
- 25 Lagergren S., and Svenska K. (1898) About of the theory of so - called adsorption of soluble substances. *Vetenskapsakad Handl.*, 24 (2) 1–39.

- 26 Ho Y.S., and McKay G. (1999) Pseudo-second order model for sorption processes. *Process Biochem.*, 34 (5) 451–465.
- 27 Chien S.H. and Clayton W.R. (1980) Application of Elovich equation to the kinetics of phosphate release and sorption in soils. *Soil Sci Soc Am J.*, 44, 265–268.
- 28 Weber W. J., and Morris J. C. (1963) Kinetics of adsorption on carbon from solution. *J. Sanit. Eng. Div., Am. Soc. Civ. Eng.*, 89 (SA2) 31–40.
- 29 Langmuir I. (1918) The adsorption of gases on plane surfaces of glass, mica and platinum. *J. Am. Chem. Soc.*, 40 (9) 1361–1403.
- 30 Freundlich H. M. F. (1906) Über die adsorption in lösungen. *Z. Phys. Chem.*, 57, 385–470.
- 31 Temkin M. J., and Pyzhev V. (1940) Recent modifications to Langmuir Isotherms. *Acta. Physicochimie USSR.*, 12, 217–222.
- 32 Dubinin M. M., and Radushkevich L. V. (1947) Equation of the Characteristic Curve of Activated Charcoal. *J. Proc. Acad. Sci. USSR, Phys. Chem.*, 55, 331–333.
- 33 Weber T. W., and Chakravorti R. K. (1974) Pore and solid diffusion models for fixed-bed adsorbers. *Am. Inst. Chem. Eng. J.*, 20 (2) 228–238.
- 34 Ho Y. S. (2006) Isotherms for the sorption of lead onto peat : Comparison of linear and non-linear methods. *Pol. J. Environ. Stud.*, 15 (1) 81–86.
- 35 Jiang L., Li S., Yu H., Zou Z., Hou X., and Shen F. (2016) Amino and thiol modified magnetic multi-walled carbon nanotubes for the simultaneous removal of lead, zinc, and phenol from aqueous solutions. *Appl. Surf. Sci.*, 369, 398–413.
- 36 Yaday L.D.S. 1st edition (2005) Organic Spectroscopy. Professor Departement of Chemistry University of Allahabad Allahabad–211 002, India.
- 37 Ho Y.S. (2006) Isotherms for the sorption of lead onto peat : Comparison of linear and non-linear methods. *P. J. Env. Studies* 15, 81–86.
- 38 Al-Anber Z.A. and Matouq M.A.D. (2008) Batch adsorption of cadmium ions from aqueous solution by means of olive cake. *J. Hazard. Mater.*, 151, 194–201.
- 39 Jiang L., Li S., Yu H., Zou Z., Hou X., Shen F., Li C. and Yao X. (2016) Amino and thiol modified magnetic multi-walled carbon nanotubes for the simultaneous removal of lead, zinc, and phenol from aqueous solutions. *Appl. Surf. Sci.*, 369, 398–413.
- 40 Singh T.S. and Pant K.K. (2004) Equilibrium, Kinetics and Thermodynamic Studies for Adsorption of As (III) on Activated Alumina. *Sep. Pur. Technol.*, 36 (2) 139–147.



© 2023 by the authors; licensee Growing Science, Canada. This is an open access article distributed under the terms and conditions of the Creative Commons Attribution (CC-BY) license (<http://creativecommons.org/licenses/by/4.0/>).